Supplement of Atmos. Chem. Phys., 26, 3299–3319, 2026
https://doi.org/10.5194/acp-26-3299-2026-supplement

Atmospheric Chemistry and Physics
Open Access
EGU

Supplement of

Aerosol-driven precipitation modification: spatiotemporal heterogeneity in precipitation microphysics and vertical profiles over China's megacity clusters

Heyuan Peng et al.

Correspondence to: Xiong Hu (huxiong18@nudt.edu.cn) and Weihua Ai (aiweihua@nudt.edu.cn)

Contents of this file

Tables. S1-S8

Figs. S1-S22

Table S1. Shallow convection statistics: event counts and percentage contributions to convective and total precipitation (analyzed in this study) across regions and seasons

Region	Season	Shallow Counts	Shallow/Conv. (%)	Shallow/Total (%)
BTH	Spring	570	13.60	1.01
	Summer	7860	30.27	5.83
	Autumn	1904	44.95	5.23
YRD	Spring	9575	57.32	8.62
	Summer	23268	53.74	13.92
	Autumn	4860	68.78	14.59
YRM	Spring	23945	41.69	6.78
	Summer	63536	51.58	13.16
	Autumn	18959	69.89	13.23
PRD	Spring	2765	37.08	9.47
	Summer	6961	46.29	20.15
	Autumn	2349	49.02	17.19

Table S2. Normalized regional differences in convective precipitation during the summer season. Units: nsRR (mm/h), STH (km), LWP (g/m^2), IWP (g/m^2).

	AOD	BTH	YRD $DIFF_{YRD}$	YRM $DIFF_{YRM}$	PRD $DIFF_{PRD}$
nsRR	[0,0.3)	5.51	8.52+54.63%	8.18+48.46%	6.96+26.32%
	[0.3,0.6)	7.18	8.7+21.17%	9.19+27.99%	7.84+9.19%
	[0.6,~)	9.57	10.62+10.97%	10.01+4.60%	4.83-49.53%
STH	[0,0.3)	8.01	9.32+16.35%	9.12+13.86%	8.86+10.61%
	[0.3,0.6)	8.4	9.13+8.69%	9.12+8.57%	9.4+11.90%
	[0.6,~)	8.78	9.4+7.06%	8.95+1.94%	9.43+7.40%
LWP	[0,0.3)	837.42	1617.55+93.16%	1518.3+81.31%	1433.93+71.23%
	[0.3,0.6)	1131.53	1710.78+51.19%	1734.55+53.29%	1509.09+33.37%
	[0.6,~)	1497.77	1996.99+33.33%	1881.02+25.59%	1108.61-25.98%
IWP	[0,0.3)	537.51	597.32+11.13%	440.41-18.06%	348.23-35.21%
	[0.3,0.6)	560.09	443.33-20.85%	466.95-16.63%	420.32-24.95%
	[0.6,~)	732.25	582.72-20.42%	414.45-43.40%	524.35-28.39%
PEI	[0,0.3)	3.92	3.24-17.35%	3.6-8.16%	3.45-11.99%
	[0.3,0.6)	3.95	3.39-14.18%	3.6-8.86%	3.36-14.94%

	[0.6,~)	3.89	3.44-11.57%	3.65-6.17%	3.09-20.57%

Table S3. Normalized regional differences in convective precipitation during the autumn season. Units: nsRR (mm/h), STH (km), LWP (g/m^2), IWP (g/m^2).

	AOD	BTH	YRD DIFF$_{YRD}$	YRM DIFF$_{YRM}$	PRD DIFF$_{PRD}$
nsRR	[0,0.3)	4.44	9.74+119.37%	7.2+62.16%	8.65+94.82%
	[0.3,0.6)	2.94	5.82+97.96%	7.87+167.69%	11.01+274.49%
	[0.6,~)	8.71	7.43-14.70%	9.58+9.99%	11.77+35.13%
STH	[0,0.3)	7.19	8.04+11.82%	8.46+17.66%	8.97+24.76%
	[0.3,0.6)	6.38	7.17+12.38%	8.24+29.15%	9.37+46.87%
	[0.6,~)	6.95	7.55+8.63%	8.31+19.57%	9.31+33.96%
LWP	[0,0.3)	613.46	1945.93+217.21%	1343.45+119.00%	1783.24+190.69%
	[0.3,0.6)	446.46	1207.72+170.51%	1431.84+220.71%	2011.4+350.52%
	[0.6,~)	1300.85	1479.28+13.72%	1799.07+38.30%	2083.57+60.17%
IWP	[0,0.3)	557.81	320.01-42.63%	281.88-49.47%	345.1-38.13%
	[0.3,0.6)	288.79	183.05-36.61%	331.64+14.84%	463.88+60.63%
	[0.6,~)	401.83	205.51-48.86%	371.5-7.55%	371.91-7.45%
PEI	[0,0.3)	3.78	3.82+1.06%	3.77-0.26%	3.57-5.56%
	[0.3,0.6)	3.82	3.56-6.81%	3.86+1.05%	3.54-7.33%
	[0.6,~)	4.48	3.82-14.73%	3.88-13.39%	3.61-19.42%

Table S4. Normalized regional differences in stratiform precipitation during the spring season. Units: nsRR (mm/h), STH (km), LWP (g/m^2), IWP (g/m^2).

	AOD	BTH	YRD DIFF$_{YRD}$	YRM DIFF$_{YRM}$	PRD DIFF$_{PRD}$
nsRR	[0,0.3)	0.93	1.36+46.24%	1.46+56.99%	3.05+227.96%
	[0.3,0.6)	1	1.62+62.00%	1.58+58.00%	2.42+142.00%
	[0.6,~)	1.3	1.94+49.23%	1.79+37.69%	2.38+83.08%
STH	[0,0.3)	4.96	6.36+28.23%	6.61+33.27%	8.85+78.43%
	[0.3,0.6)	5.06	6.21+22.73%	6.12+20.95%	8.23+62.65%
	[0.6,~)	5.09	6.13+20.43%	6.19+21.61%	6.59+29.47%
LWP	[0,0.3)	95.98	333.27+247.23%	315.85+229.08%	690.6+619.52%
	[0.3,0.6)	110.85	356.54+221.64%	289.78+161.42%	574.41+418.19%
	[0.6,~)	183.89	390.26+112.22%	339.58+84.66%	482.9+162.60%
IWP	[0,0.3)	144.8	209.34+44.57%	210.08+45.08%	446.22+208.16%
	[0.3,0.6)	153.29	210.26+37.16%	197.12+28.59%	369.52+141.06%
	[0.6,~)	191.16	245.43+28.39%	217.98+14.03%	256.4+34.13%
PEI	[0,0.3)	4.02	2.49-38.06%	2.86-28.86%	2.29-43.03%
	[0.3,0.6)	4.02	2.74-31.84%	3.3-17.91%	2.34-41.79%
	[0.6,~)	3.79	2.92-22.96%	3.24-14.51%	2.85-24.80%

Table S5. Normalized regional differences in stratiform precipitation during the summer season. Units: nsRR (mm/h), STH (km), LWP (g/m^2), IWP (g/m^2).

	AOD	BTH	YRD $DIFF_{YRD}$	YRM $DIFF_{YRM}$	PRD $DIFF_{PRD}$
nsRR	[0,0.3)	1.22	2.02+65.57%	1.86+52.46%	1.61+31.97%
	[0.3,0.6)	1.49	2+34.23%	1.94+30.20%	2.01+34.90%
	[0.6,~)	1.7	2.19+28.82%	1.92+12.94%	1.73+1.76%
STH	[0,0.3)	6.54	7.54+15.29%	7.51+14.83%	7.97+21.87%
	[0.3,0.6)	6.8	7.52+10.59%	7.45+9.56%	8.11+19.26%
	[0.6,~)	6.84	7.61+11.26%	7.18+4.97%	8.05+17.69%
LWP	[0,0.3)	257.08	506.57+97.05%	427.8+66.41%	427.38+66.24%
	[0.3,0.6)	315.9	500.38+58.40%	452.6+43.27%	515.3+63.12%
	[0.6,~)	360.3	538.54+49.47%	455.06+26.30%	434.75+20.66%
IWP	[0,0.3)	182.12	279.9+53.69%	242.59+33.20%	250.67+37.64%
	[0.3,0.6)	228.45	276.69+21.12%	243.63+6.64%	293.8+28.61%
	[0.6,~)	264.35	268.24+1.47%	223.43-15.48%	272.26+2.99%
PEI	[0,0.3)	2.91	2.31-20.62%	2.62-9.97%	2.31-20.62%
	[0.3,0.6)	2.66	2.34-12.03%	2.59-2.63%	2.28-14.29%
	[0.6,~)	2.63	2.43-7.60%	2.55-3.04%	2.34-11.03%

Table S6. Normalized regional differences in stratiform precipitation during the autumn season. Units: nsRR (mm/h), STH (km), LWP (g/m^2), IWP (g/m^2).

	AOD	BTH	YRD $DIFF_{YRD}$	YRM $DIFF_{YRM}$	PRD $DIFF_{PRD}$
nsRR	[0,0.3)	1.08	1.7+57.41%	1.6+48.15%	3.41+215.74%
	[0.3,0.6)	0.98	1.69+72.45%	1.74+77.55%	2.83+188.78%
	[0.6,~)	1.43	1.78+24.48%	1.88+31.47%	3.59+151.05%
STH	[0,0.3)	6.05	7.03+16.20%	6.85+13.22%	8.1+33.88%
	[0.3,0.6)	5.83	6.72+15.27%	6.9+18.35%	8.04+37.91%
	[0.6,~)	5.68	6.96+22.54%	6.9+21.48%	8.03+41.37%
LWP	[0,0.3)	198.21	411.77+107.74%	351.75+77.46%	780.62+293.83%
	[0.3,0.6)	199.89	415.63+107.93%	382.88+91.55%	660.45+230.41%
	[0.6,~)	186.38	439.71+135.92%	418.06+124.31%	812.36+335.86%
IWP	[0,0.3)	236.27	208.2-11.88%	203.79-13.75%	373.67+58.15%
	[0.3,0.6)	155.5	199.16+28.08%	208.03+33.78%	331.96+113.48%
	[0.6,~)	186.38	223.12+19.71%	224.35+20.37%	360.32+93.33%
PEI	[0,0.3)	2.8	2.51-10.36%	2.86+2.14%	2.53-9.64%
	[0.3,0.6)	2.82	2.57-8.87%	2.86+1.42%	2.36-16.31%
	[0.6,~)	3.1	2.52-18.71%	2.86-7.74%	2.73-11.94%

Table S7. Normalized seasonal differences in convective precipitation during the summer season. Units: nsRR (mm/h), STH (km), LWP (g/m^2), IWP (g/m^2).

	AOD	BTH DIFF$_{summer}$	YRD DIFF$_{summer}$	YRM DIFF$_{summer}$	PRD DIFF$_{summer}$	BTH DIFF$_{autumn}$	YRD DIFF$_{autumn}$	YRM DIFF$_{autumn}$	PRD DIFF$_{autumn}$
nsRR	[0,0.3)	5.51+83.67%	8.52+101.42%	8.18-21.50%	6.96-67.48%	4.44+48.00%	9.74+130.26%	7.2-30.90%	8.65-59.58%
	[0.3,0.6)	7.18+122.29%	8.7-4.40%	9.19+18.58%	7.84-33.33%	2.94-8.98%	5.82-36.04%	7.87+1.55%	11.01-6.38%
	[0.6,~)	9.57+54.60%	10.62+6.09%	10.01+8.10%	4.83-69.47%	8.71+40.71%	7.43-25.77%	9.58+3.46%	11.77-25.60%
STH	[0,0.3)	8.01+14.59%	9.32+33.72%	9.12+2.82%	8.86-14.40%	7.19+2.86%	8.04+15.35%	8.46-4.62%	8.97-13.33%
	[0.3,0.6)	8.4+23.71%	9.13+22.39%	9.12+14.00%	9.4-3.89%	6.38-6.04%	7.17-3.89%	8.24+3.00%	9.37-4.19%
	[0.6,~)	8.78+22.45%	9.4+26.34%	8.95+12.86%	9.43+5.60%	6.95-3.07%	7.55+1.48%	8.31+4.79%	9.31+4.26%
LWP	[0,0.3)	837.42+135.82%	1617.55+81.25%	1518.3-4.72%	1433.93-59.05%	613.46+72.75%	1945.93+118.05%	1343.45-15.70%	1783.24-49.08%
	[0.3,0.6)	1131.53+172.94%	1710.78+5.41%	1734.55+39.56%	1509.09-25.29%	446.46+7.69%	1207.72-25.59%	1431.84+15.20%	2011.4-0.42%
	[0.6,~)	1497.77+95.79%	1996.99+21.83%	1881.02+32.90%	1108.61-53.96%	1300.85+70.05%	1479.28-9.76%	1799.07+27.11%	2083.57-13.47%
IWP	[0,0.3)	537.51-8.06%	597.32+199.98%	440.41-26.15%	348.23-56.50%	557.81-4.58%	320.01+60.71%	281.88-52.73%	345.1-56.89%
	[0.3,0.6)	560.09+20.05%	443.33+38.92%	466.95+22.48%	420.32-23.88%	288.79-38.10%	183.05-42.64%	331.64-13.01%	463.88-15.99%
	[0.6,~)	732.25+41.16%	582.72+60.88%	414.45-1.20%	524.35-23.48%	401.83-22.53%	205.51-43.26%	371.5-11.44%	371.91-45.73%
PEI	[0,0.3)	3.92+5.95%	3.24-7.16%	3.6-10.22%	3.45-17.27%	3.78+2.16%	3.82+9.46%	3.77-5.99%	3.57-14.39%
	[0.3,0.6)	3.95-1.50%	3.39-13.08%	3.6-14.49%	3.36-10.40%	3.82-4.74%	3.56-8.72%	3.86-8.31%	3.54-5.60%
	[0.6,~)	3.89-15.62%	3.44-19.44%	3.65-16.48%	3.09-28.64%	4.48-2.82%	3.82-10.54%	3.88-11.21%	3.61-16.63%

Table S8. Normalized seasonal differences in stratiform precipitation during the summer season. Units: nsRR (mm/h), STH (km), LWP (g/m^2), IWP (g/m^2).

	AOD	BTH DIFF$_{summer}$	YRD DIFF$_{summer}$	YRM DIFF$_{summer}$	PRD DIFF$_{summer}$	BTH DIFF$_{autumn}$	YRD DIFF$_{autumn}$	YRM DIFF$_{autumn}$	PRD DIFF$_{autumn}$
nsRR	[0,0.3)	1.22+31.18%	2.02+48.53%	1.86+27.40%	1.61-47.21%	1.08+16.13%	1.7+25.00%	1.6+9.59%	3.41+11.80%
	[0.3,0.6)	1.49+49.00%	2+23.46%	1.94+22.78%	2.01-16.94%	0.98-2.00%	1.69+4.32%	1.74+10.13%	2.83+16.94%
	[0.6,~)	1.7+30.77%	2.19+12.89%	1.92+7.26%	1.73-27.31%	1.43+10.00%	1.78-8.25%	1.88+5.03%	3.59+50.84%
STH	[0,0.3)	6.54+31.85%	7.54+18.55%	7.51+13.62%	7.97-9.94%	6.05+21.98%	7.03+10.53%	6.85+3.63%	8.1-8.47%
	[0.3,0.6)	6.8+34.39%	7.52+21.10%	7.45+21.73%	8.11-1.46%	5.83+15.22%	6.72+8.21%	6.9+12.75%	8.04-2.31%
	[0.6,~)	6.84+34.38%	7.61+24.14%	7.18+15.99%	8.05+22.15%	5.68+11.59%	6.96+13.54%	6.9+11.47%	8.03+21.85%
LWP	[0,0.3)	257.08+167.85%	506.57+52.00%	427.8+35.44%	427.38-38.11%	198.21+106.51%	411.77+23.55%	351.75+11.37%	780.62+13.04%
	[0.3,0.6)	315.9+184.98%	500.38+40.34%	452.6+56.19%	515.3-10.29%	199.89+80.32%	415.63+16.57%	382.88+32.13%	660.45+14.98%
	[0.6,~)	360.3+95.93%	538.54+38.00%	455.06+34.01%	434.75-9.97%	186.38+1.35%	439.71+12.67%	418.06+23.11%	812.36+68.23%
IWP	[0,0.3)	182.12+25.77%	279.9+33.71%	242.59+15.48%	250.67-43.82%	236.27+63.17%	208.2-0.54%	203.79-2.99%	373.67-16.26%
	[0.3,0.6)	228.45+49.03%	276.69+31.59%	243.63+23.59%	293.8-20.49%	155.5+1.44%	199.16-5.28%	208.03+5.53%	331.96-10.16%
	[0.6,~)	264.35+38.29%	268.24+9.29%	223.43+2.50%	272.26+6.19%	186.38-2.50%	223.12-9.09%	224.35+2.92%	360.32+40.53%
PEI	[0,0.3)	2.91-27.61%	2.31-7.23%	2.62-8.39%	2.31+0.87%	2.8-30.35%	2.51+0.80%	2.86+0.00%	2.53+10.48%
	[0.3,0.6)	2.66-33.83%	2.34-14.60%	2.59-21.52%	2.28-2.56%	2.82-29.85%	2.57-6.20%	2.86-13.33%	2.36+0.85%
	[0.6,~)	2.63-30.61%	2.43-16.78%	2.55-21.30%	2.34-17.89%	3.1-18.21%	2.52-13.70%	2.86-11.73%	2.73-4.21%

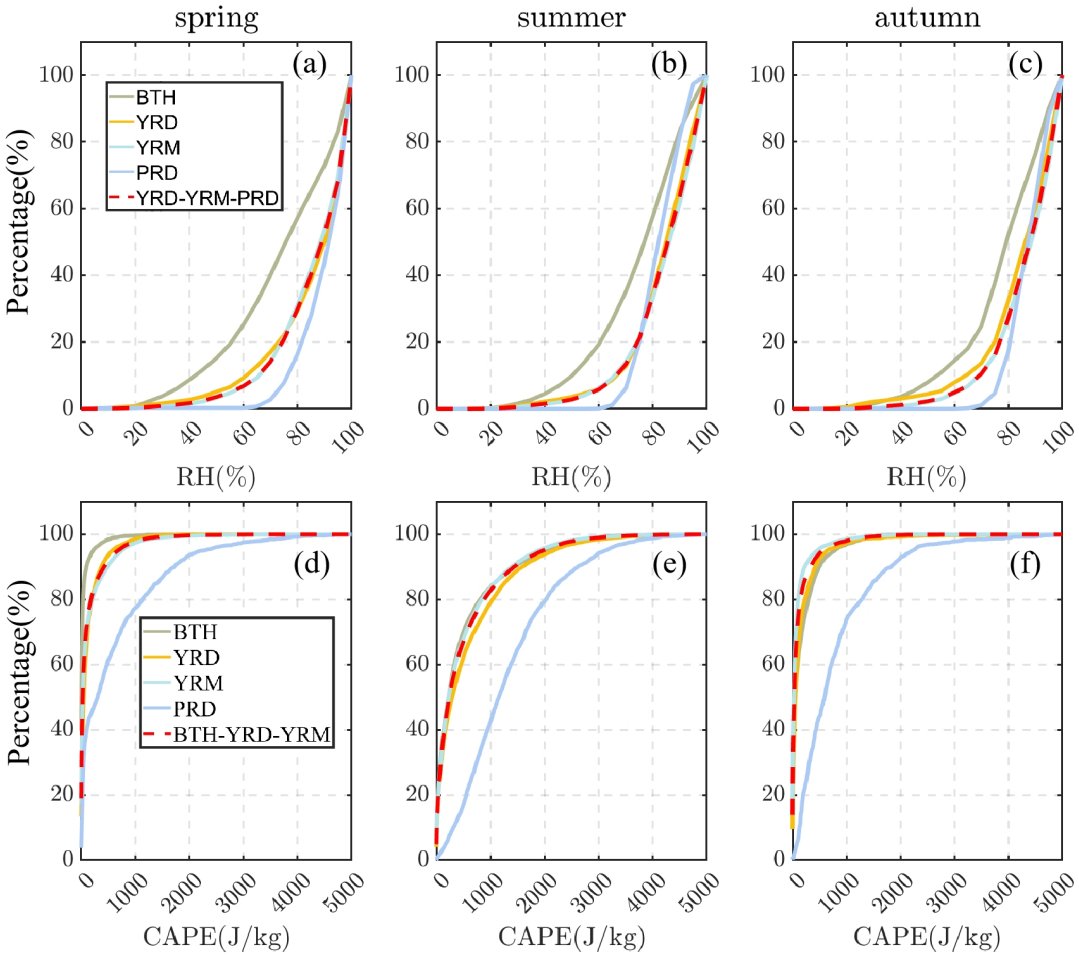

Fig. S1. Cumulative Distribution Functions (CDFs) of RH and CAPE for different regions in the three seasons. The gray-green curve represents the BTH, yellow-YRD, green-YRM, and blue-PRD. For RH (a-c), the red dashed line shows the CDF after merging data from YRD, YRM, and PRD; for CAPE (d-f), the red dashed line shows the CDF after merging data from BTH, YRD, and YRM.

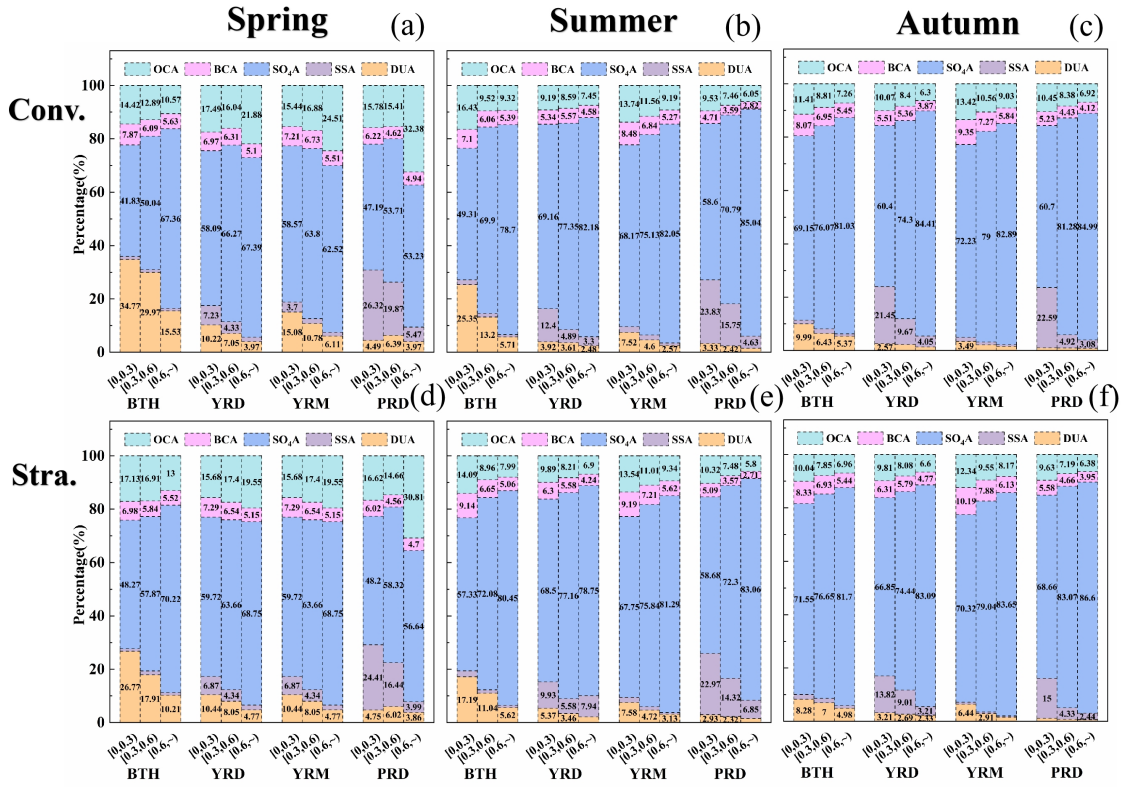

Fig. S2. Proportion of AOD in convective precipitation and stratiform precipitation under different AOD loads in spring, summer, and autumn in the four regions.

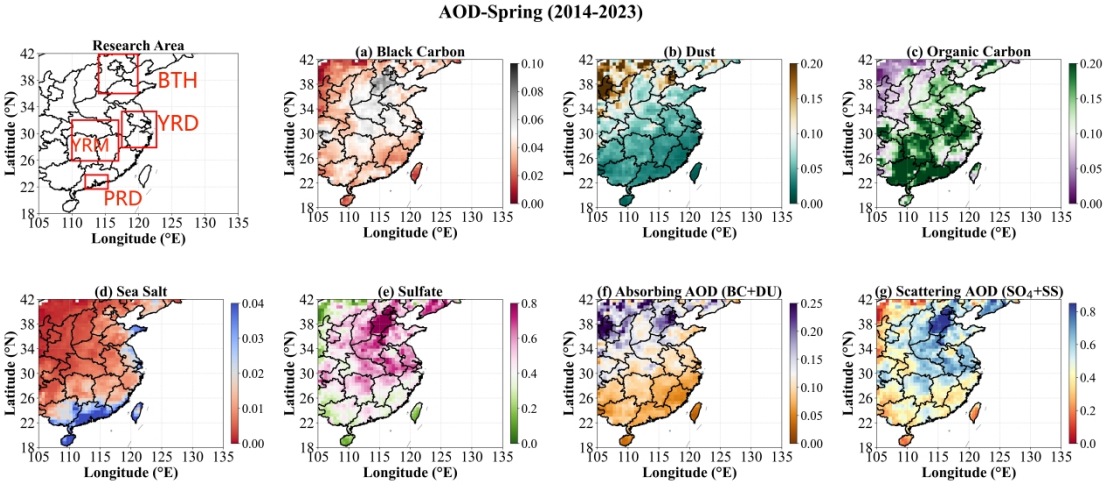

Fig. S3. Spatial distribution map of seven types (BC, DU, OC, SS, SO_4, absorbing, and scattering) of average aerosols in spring from 2014 to 2023 over China's Megacity Clusters (BTH, YRD, YRM, and PRD).

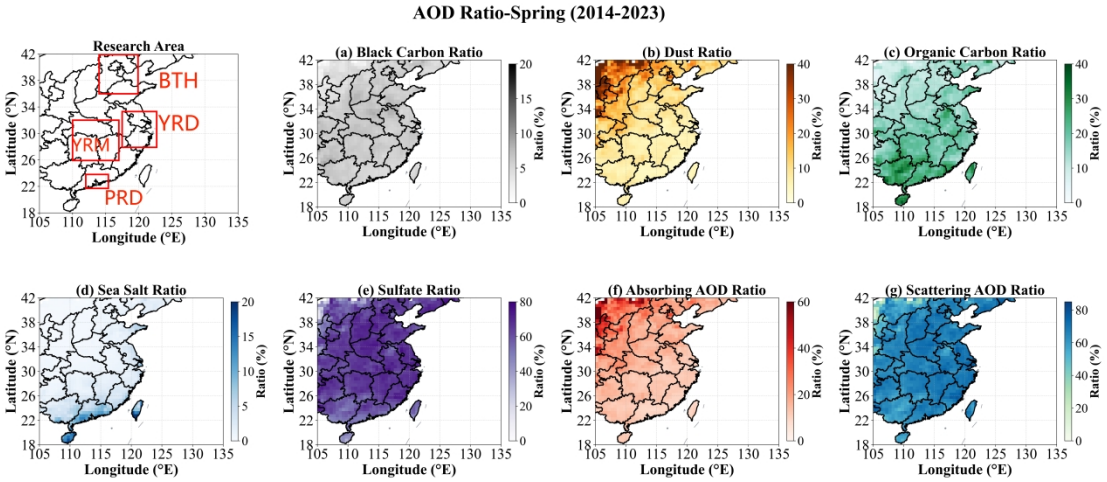

Fig. S4. Spatial distribution map of seven types (BC, DU, OC, SS, SO_4, absorbing, and scattering) of aerosol type proportions in spring from 2014 to 2023 over China's Megacity Clusters (BTH, YRD, YRM, and PRD).

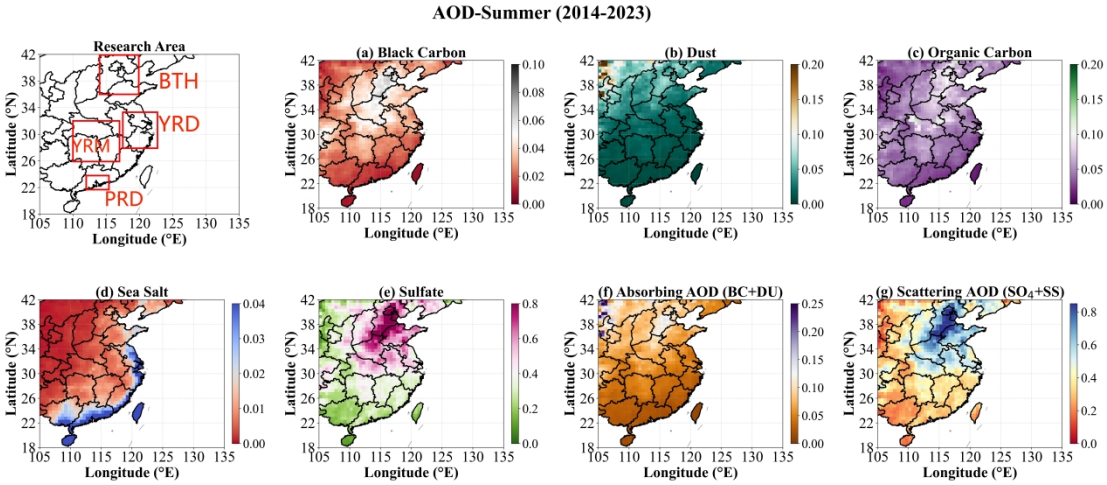

Fig. S5. Spatial distribution map of seven types (BC, DU, OC, SS, SO_4, absorbing, and scattering) of average aerosols in summer from 2014 to 2023 over China's Megacity Clusters (BTH, YRD, YRM, and PRD).

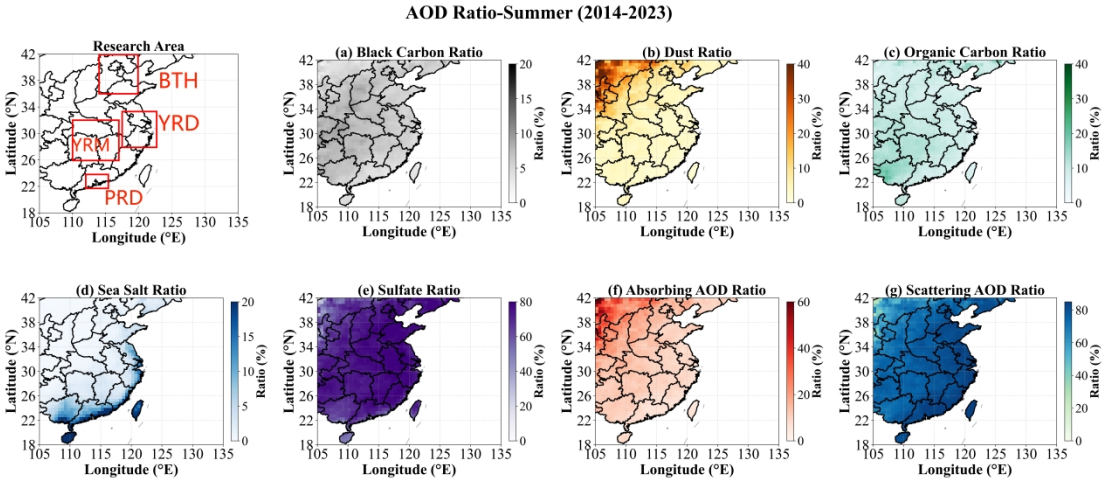

Fig. S6. Spatial distribution map of seven types (BC, DU, OC, SS, SO_4, absorbing, and scattering) of aerosol type proportions in summer from 2014 to 2023 over China's Megacity Clusters (BTH, YRD, YRM, and PRD).

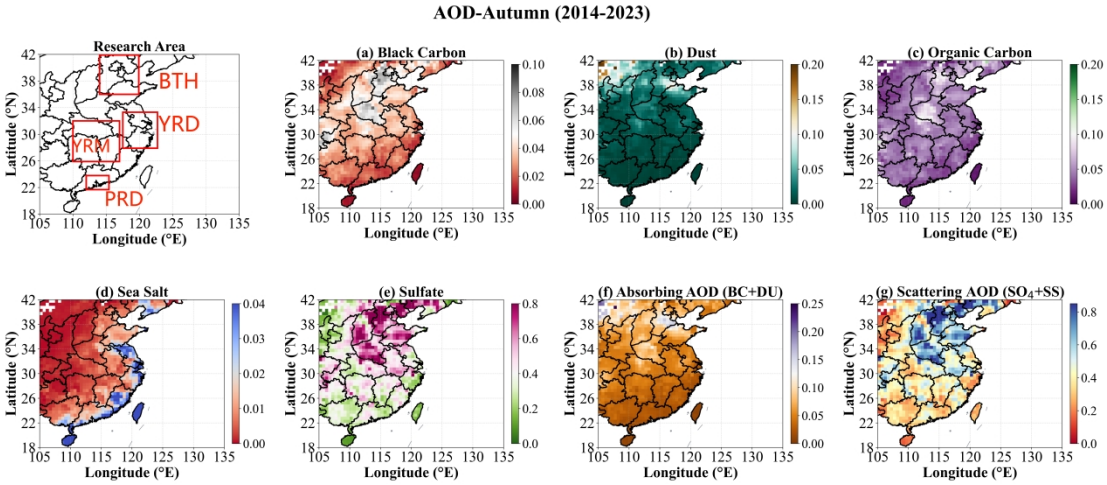

Fig. S7. Spatial distribution map of seven types (BC, DU, OC, SS, SO_4, absorbing, and scattering) of average aerosols in autumn from 2014 to 2023 over China's Megacity Clusters (BTH, YRD, YRM, and PRD).

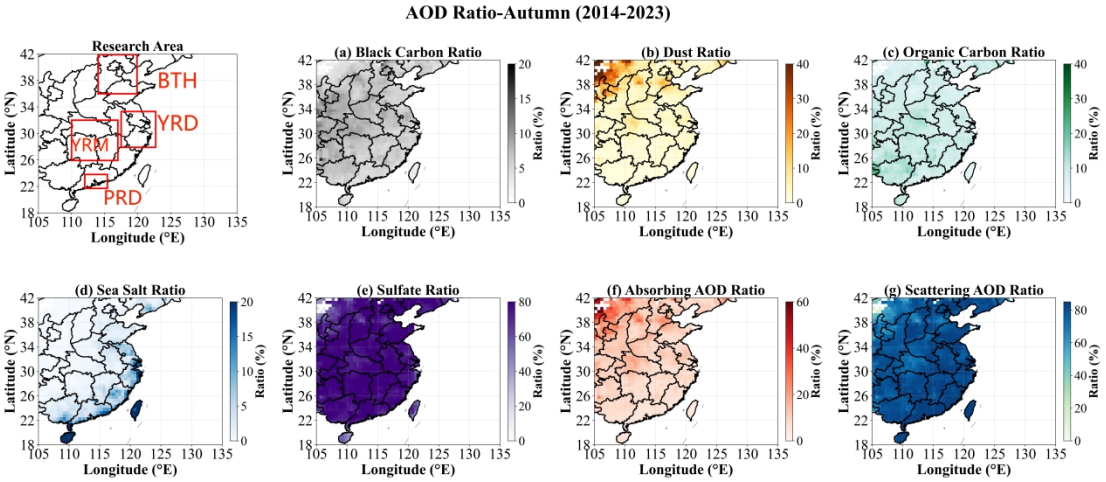

Fig. S8. Spatial distribution map of seven types (BC, DU, OC, SS, SO_4, absorbing, and scattering) of aerosol type proportions in autumn from 2014 to 2023 over China's Megacity Clusters (BTH, YRD, YRM, and PRD).

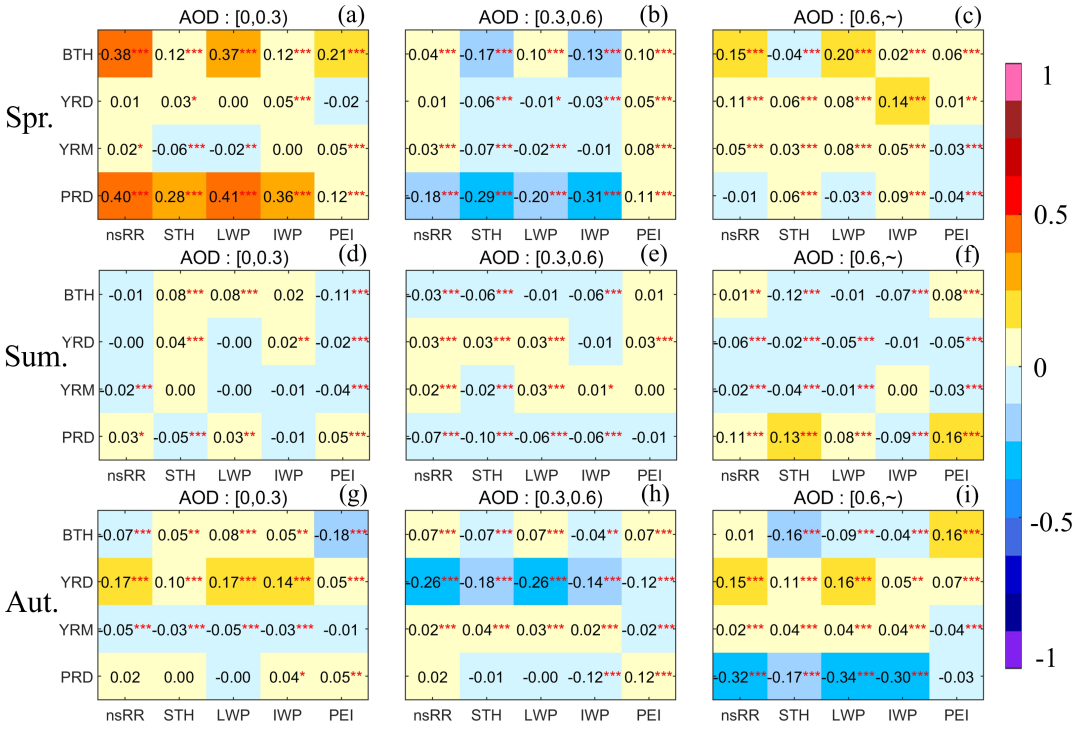

Fig. S9. Spearman correlation coefficients between AOD and precipitation parameters (nsRR, STH, LWP, IWP, and PEI) for stratiform precipitation across regions and

seasons under three AOD regimes. The form of this expression is similar to that shown in Figure 2.

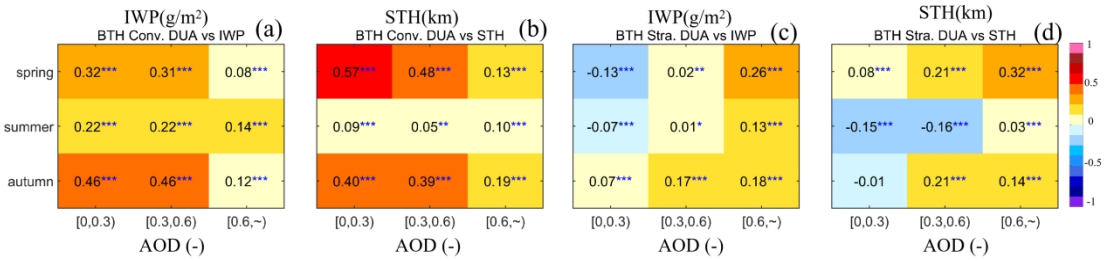

Fig. S10. Spearman correlation coefficients between DUA and precipitation parameters (STH, and IWP) in BTH for convective and stratiform precipitation under three AOD regimes and seasons.

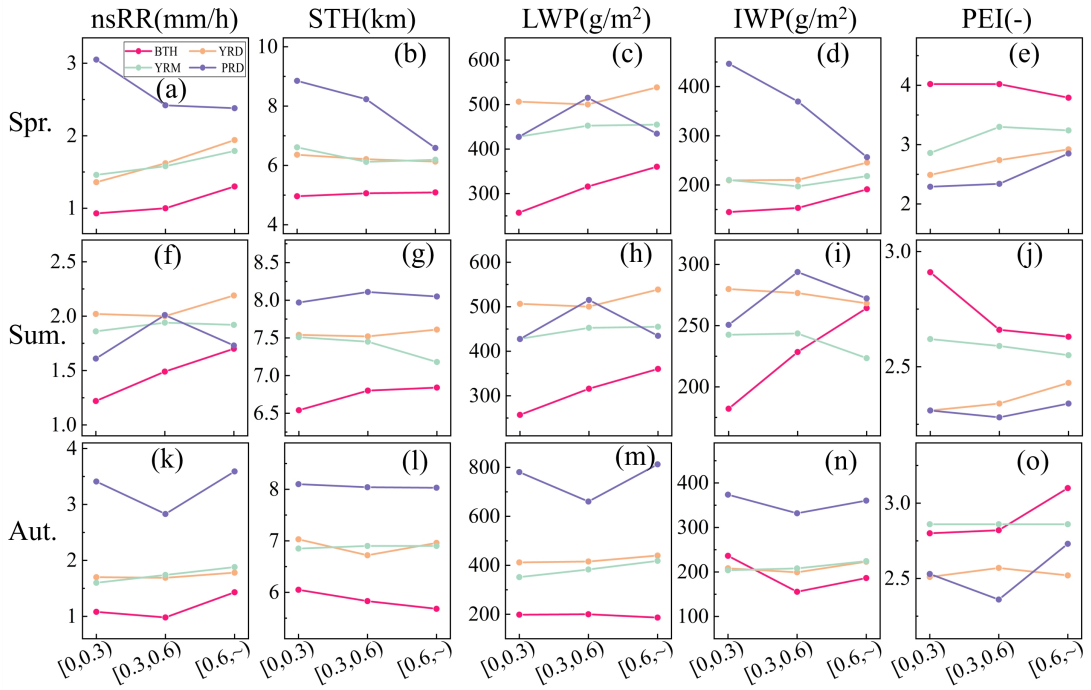

Fig. S11. Average point line plots of nsRR, STH, LWP, IWP, and PEI under the three AOD conditions for stratiform precipitation across various regions and seasons. The form of the expression is similar to that shown in Fig. 3. "-" indicates dimensionless (after scaling by 1000).

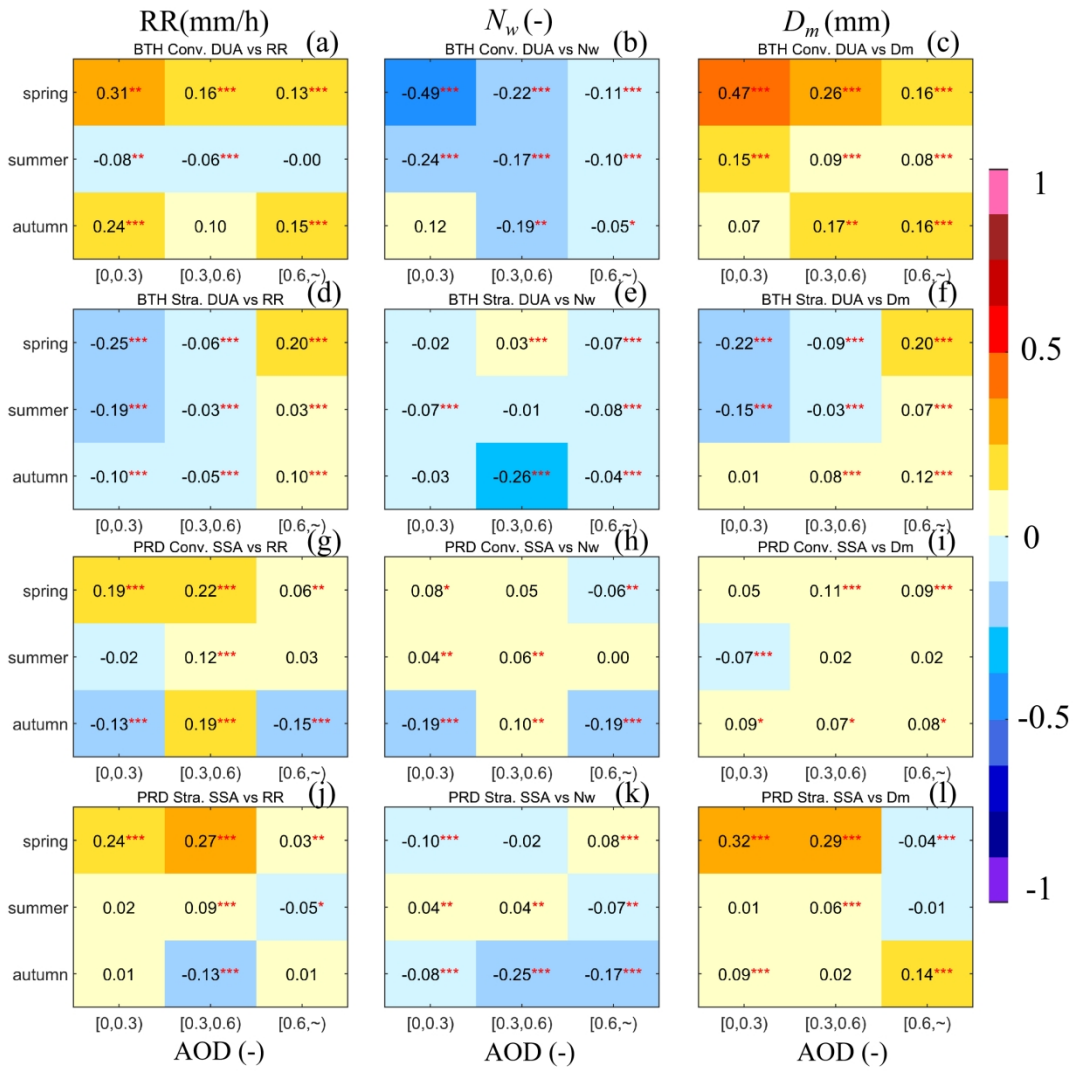

Fig. S12. Spearman correlation coefficients between key aerosol types (DUA for the BTH and SSA for the PRD) and precipitation parameters (RR, N_w and D_m) across regions and seasons under the three AOD regimes. Color gradients (from yellow to blue) encode the correlation strength and direction, and asterisks denote statistical significance (*：p<0.05, **：p<0.01, ***：p<0.001).

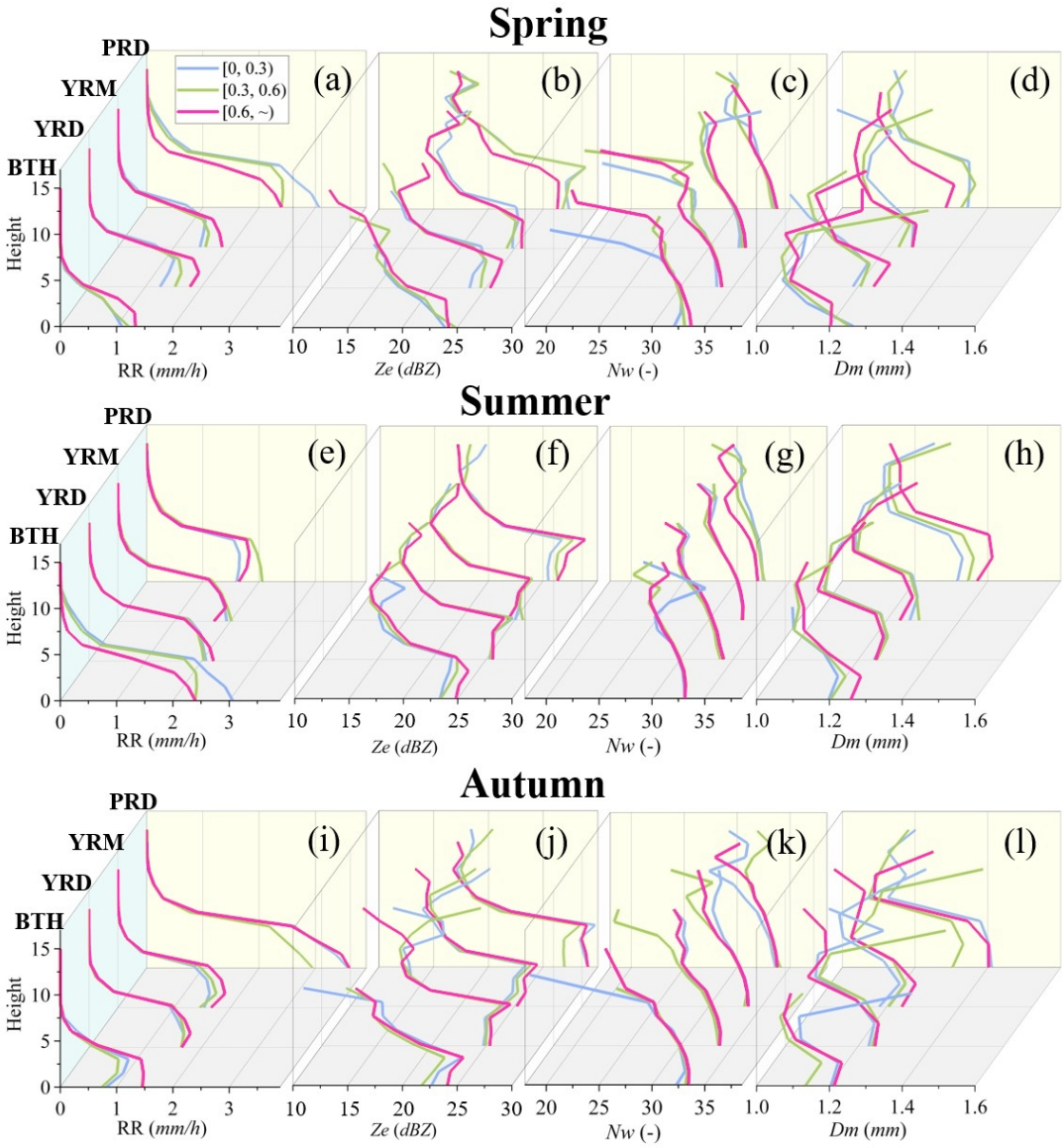

Fig .S13. Vertical profiles of the average stratiform precipitation parameters Z_e, D_m, N_w, and RR for different regions in different seasons under three AOD conditions. The form of this expression is similar to that shown in Fig. 4.

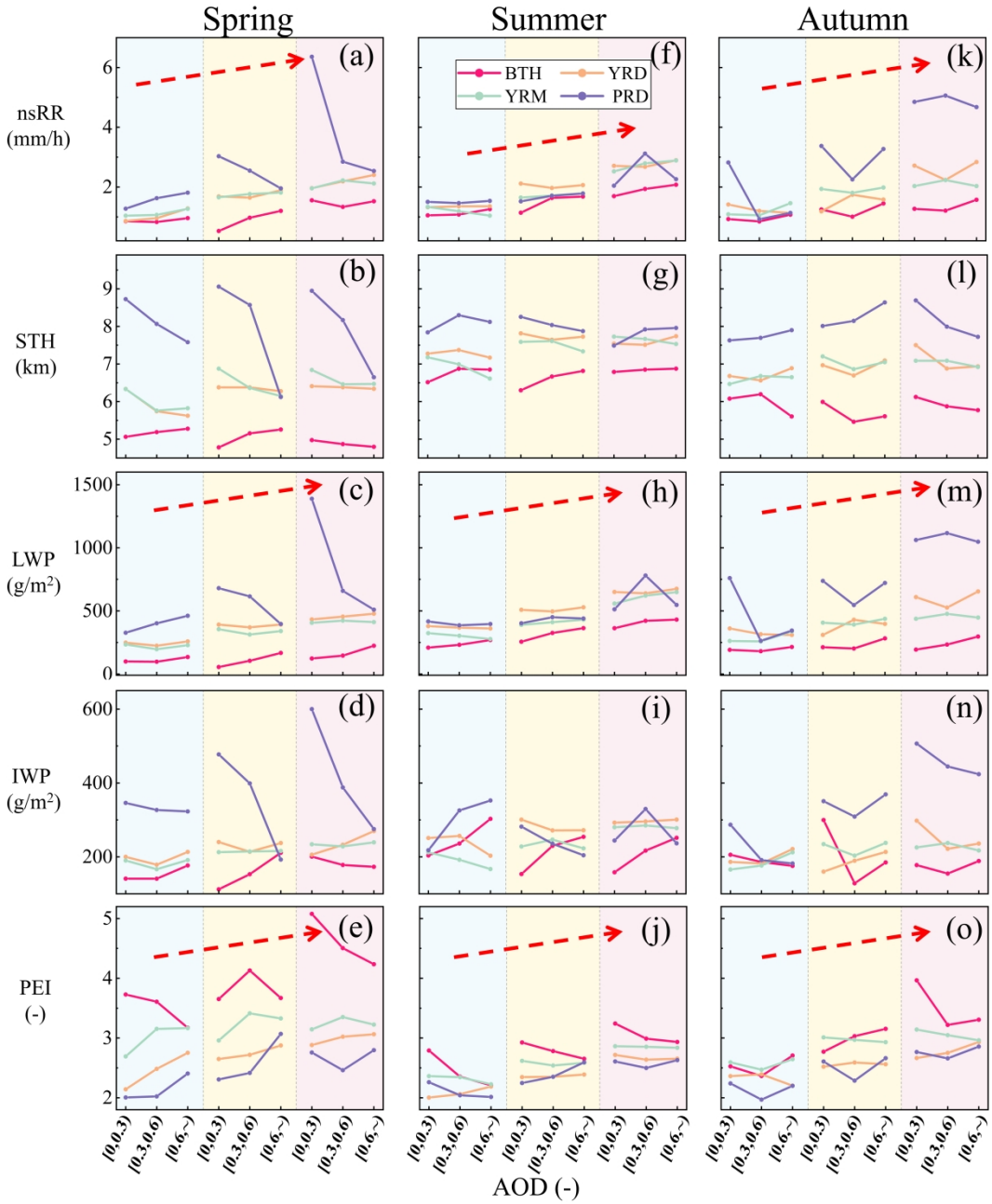

Fig. S14. Point-line graphs of mean values for stratiform precipitation parameters across seasons and regions. The analysis is based on three AOD intervals and various RH scenarios. The form of this expression is similar to that shown in Fig. 7.

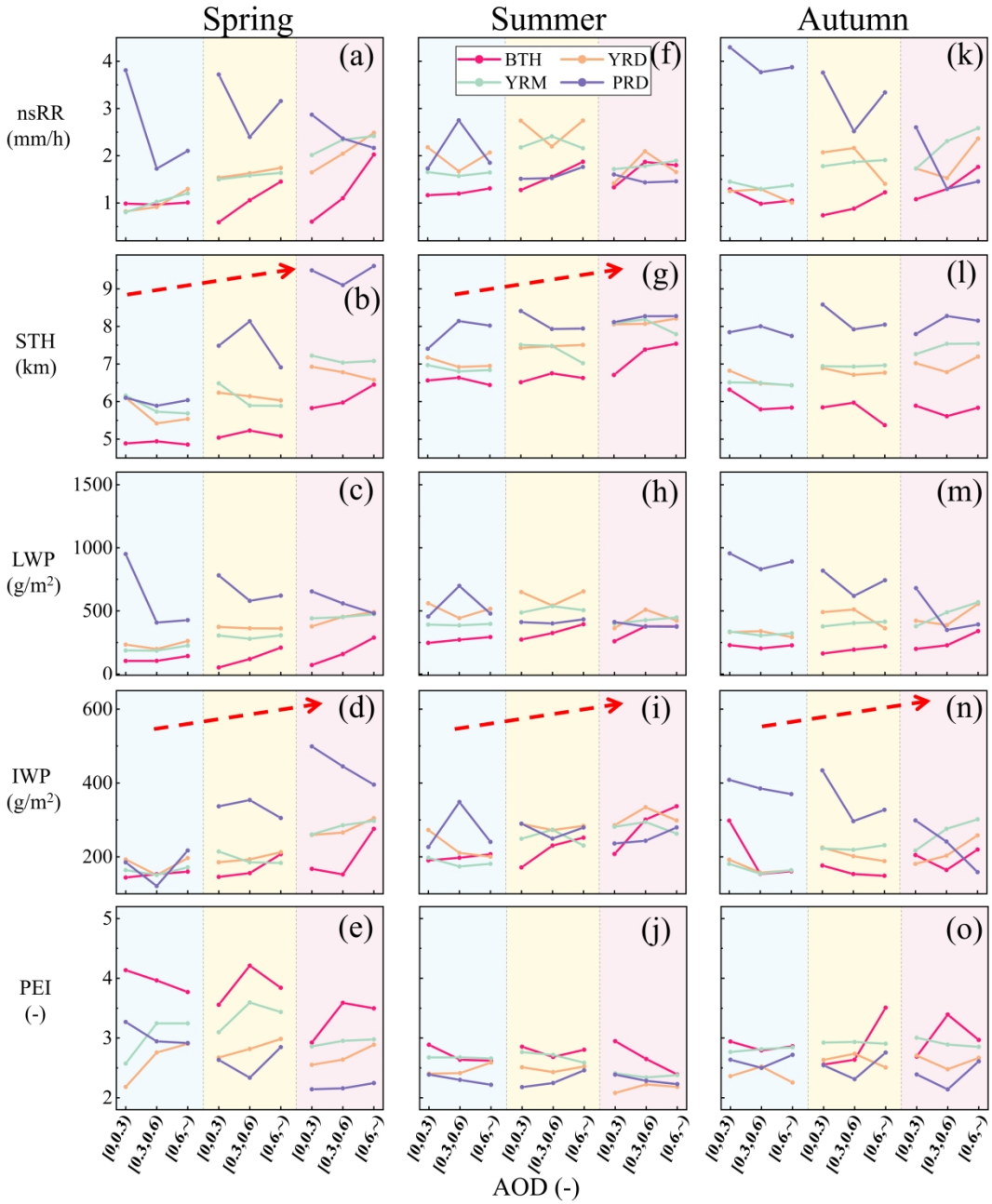

Fig. S15. Point-line graphs of mean values for stratiform precipitation parameters across seasons and regions. The analysis is based on three AOD intervals and the CAPE scenarios. The form of expression is similar to Fig. 7.

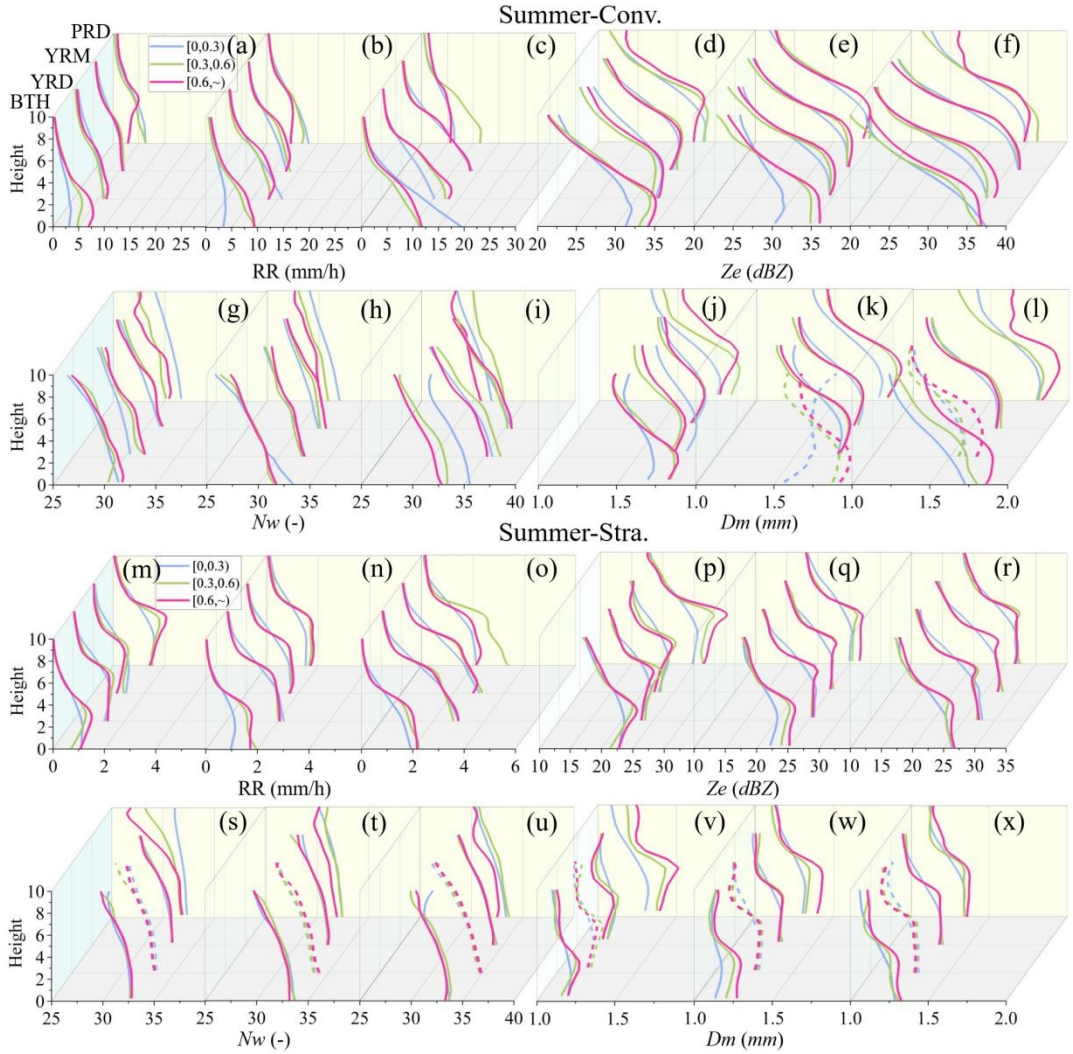

Fig. S16. Vertical profiles of mean precipitation parameters for convective and stratiform precipitation in summer across the four regions. The profiles are shown for the three AOD scenarios and RH conditions. The form of this expression is similar to that shown in Fig. 9.

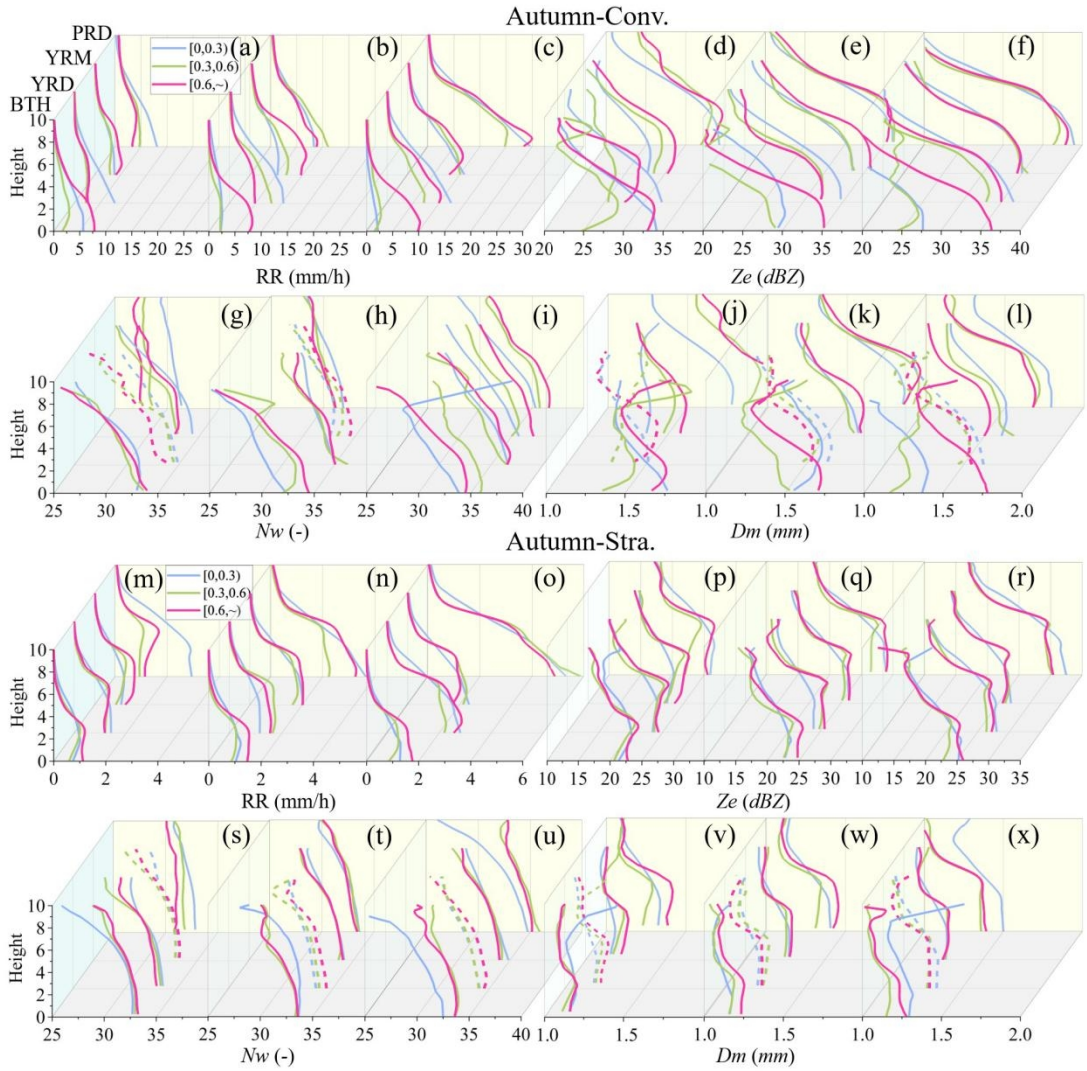

Fig. S17. Vertical profiles of mean precipitation parameters for convective and stratiform precipitation in autumn across the four regions. The profiles are shown for the three AOD scenarios and RH conditions. The form of this expression is similar to that shown in Fig. 9.

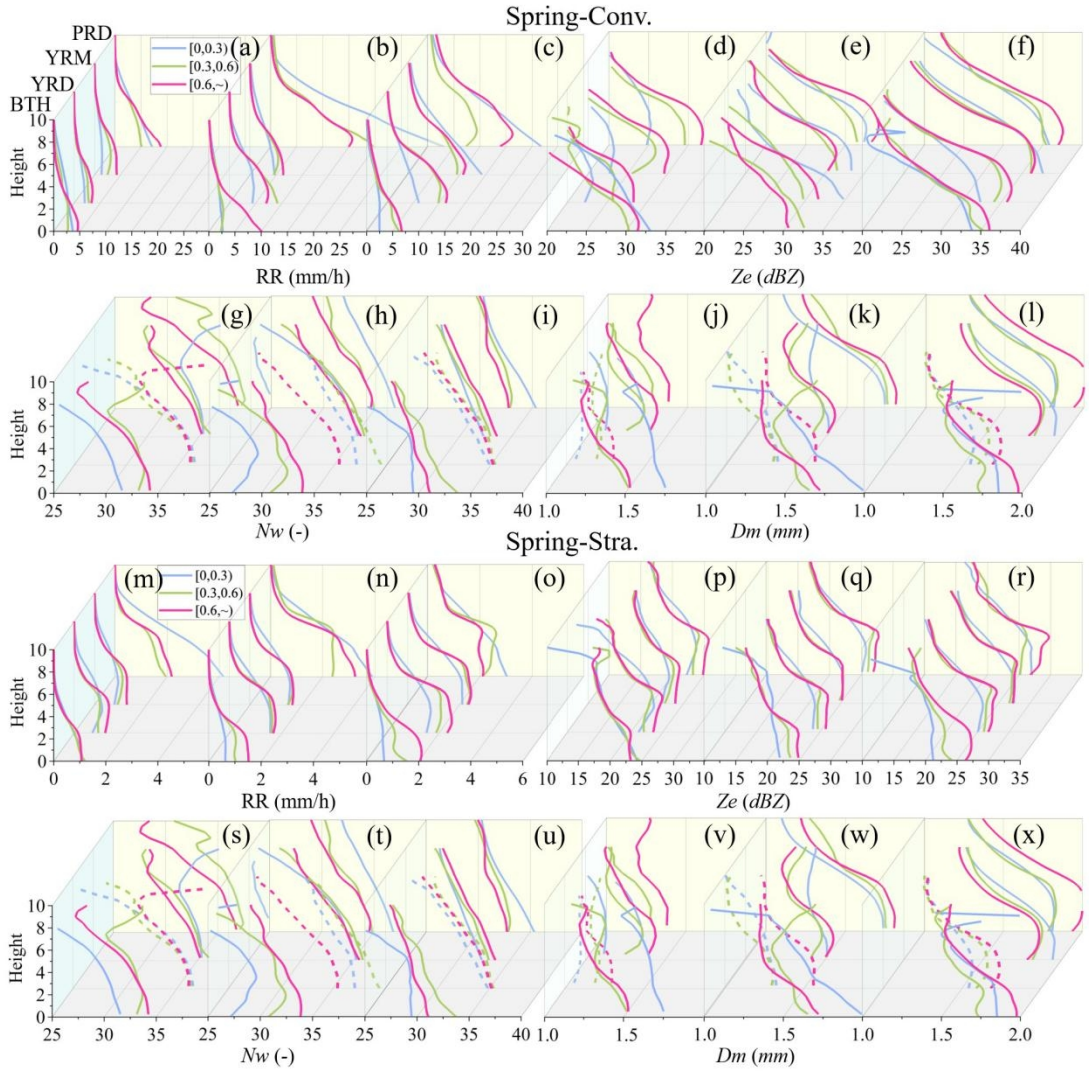

Fig. S18. Vertical profiles of mean precipitation parameters for convective and stratiform precipitation in spring across the four regions. The profiles are shown under three AOD and CAPE scenarios. The form of this expression is similar to that shown in Fig. 9.

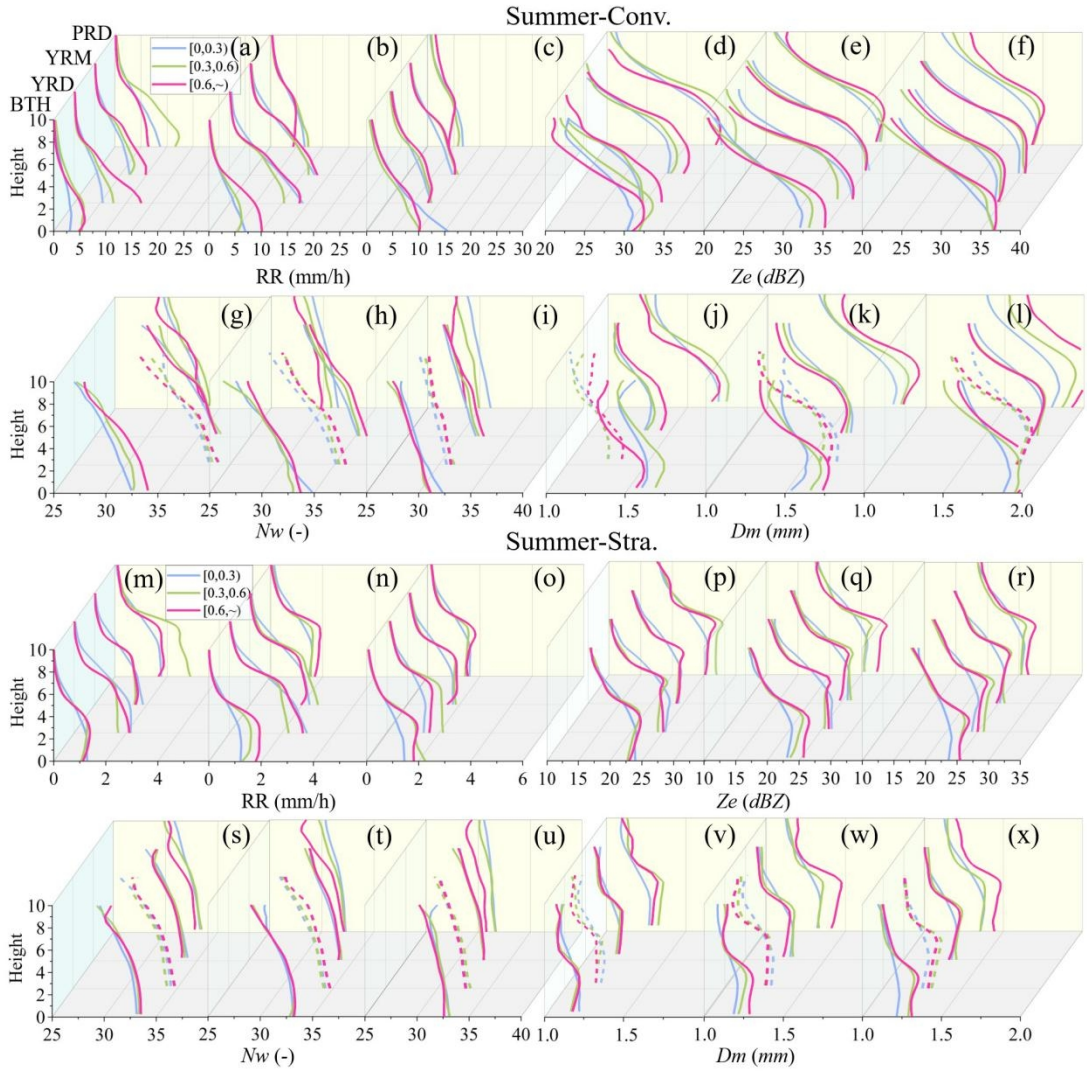

Fig. S19. Vertical profiles of mean precipitation parameters for convective and stratiform precipitation in summer across four regions. The profiles are shown under three AOD scenarios and CAPE conditions. as solid lines. The form of this expression is similar to that shown in Fig. 9.

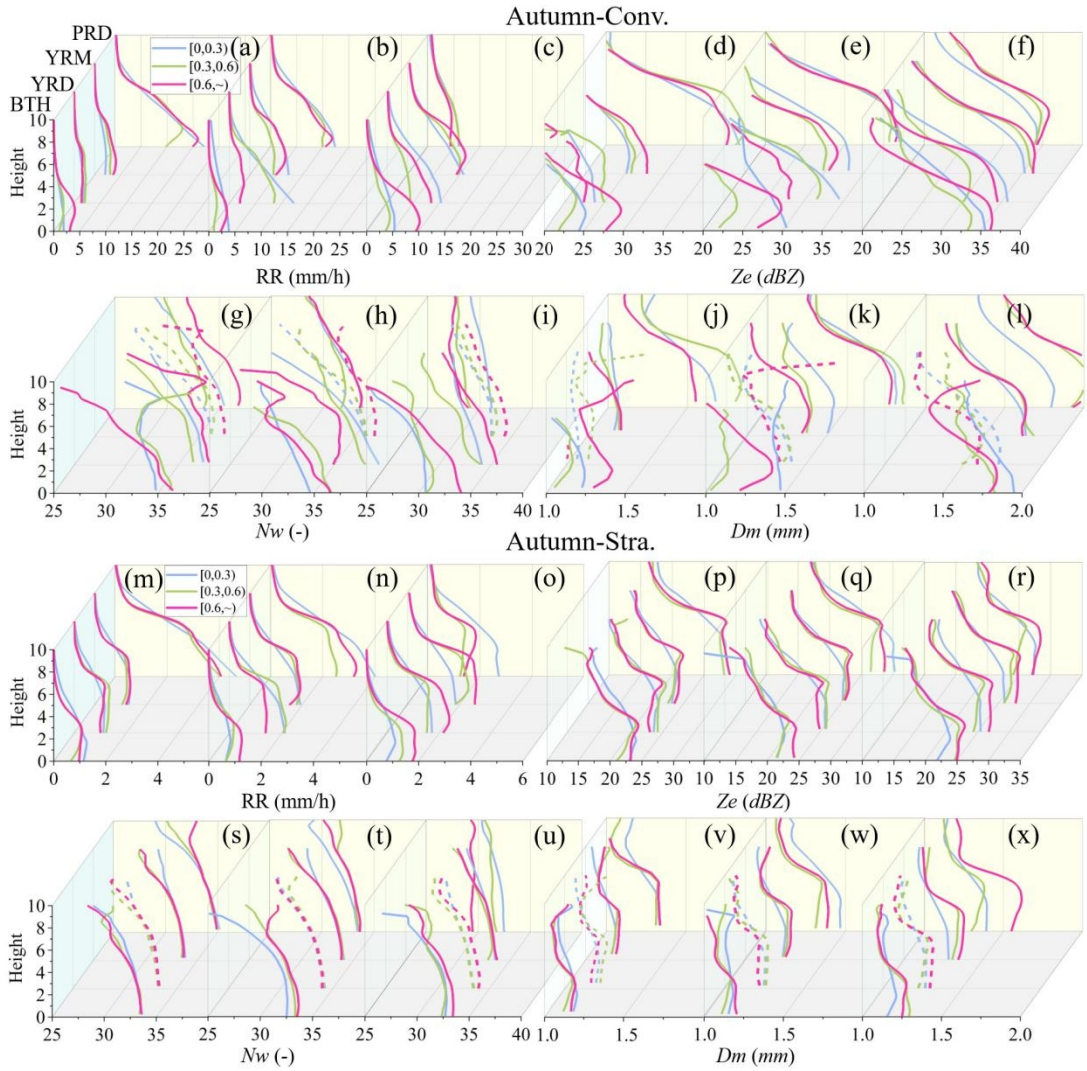

Fig. S20. Vertical profiles of mean precipitation parameters for convective and stratiform precipitation in autumn across four regions. The profiles are shown under three AOD scenarios and CAPE conditions. as solid lines. The form of this expression is similar to that shown in Fig. 9.

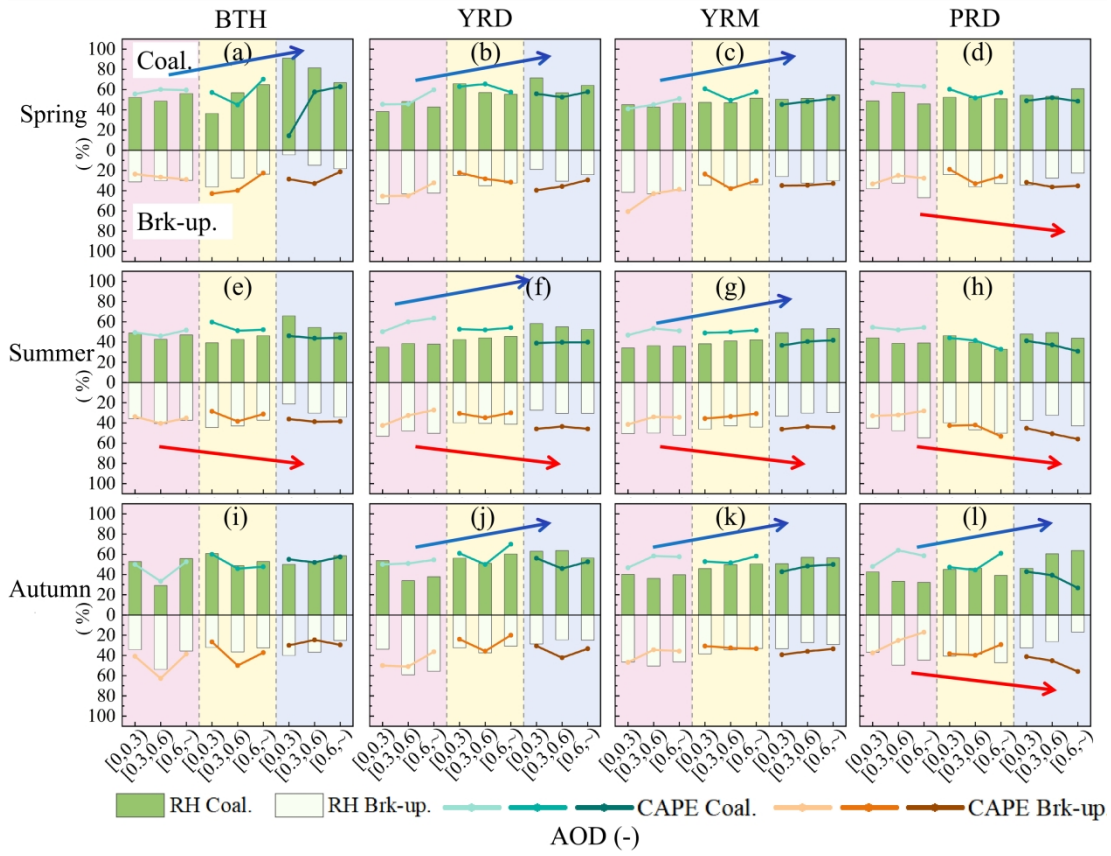

Fig. S21. Convective precipitation coalescence and break-up processes under varying RH and CAPE conditions in spring (a–d), summer (e–h), and autumn (i–l) across regions sorted by AOD loading. Each subpanel is split as follows: upper for the coalescence proportion and lower for the break-up proportion. The bar charts show RH variations under different AODs, and the line charts show CAPE variations. Meteorological conditions (left to right): low (pink background), medium (yellow background), and high (blue background) RH, and CAPE. The blue arrows indicate increasing coalescence proportions as RH rises, whereas the red arrows denote growing break-up proportions with enhanced CAPE.

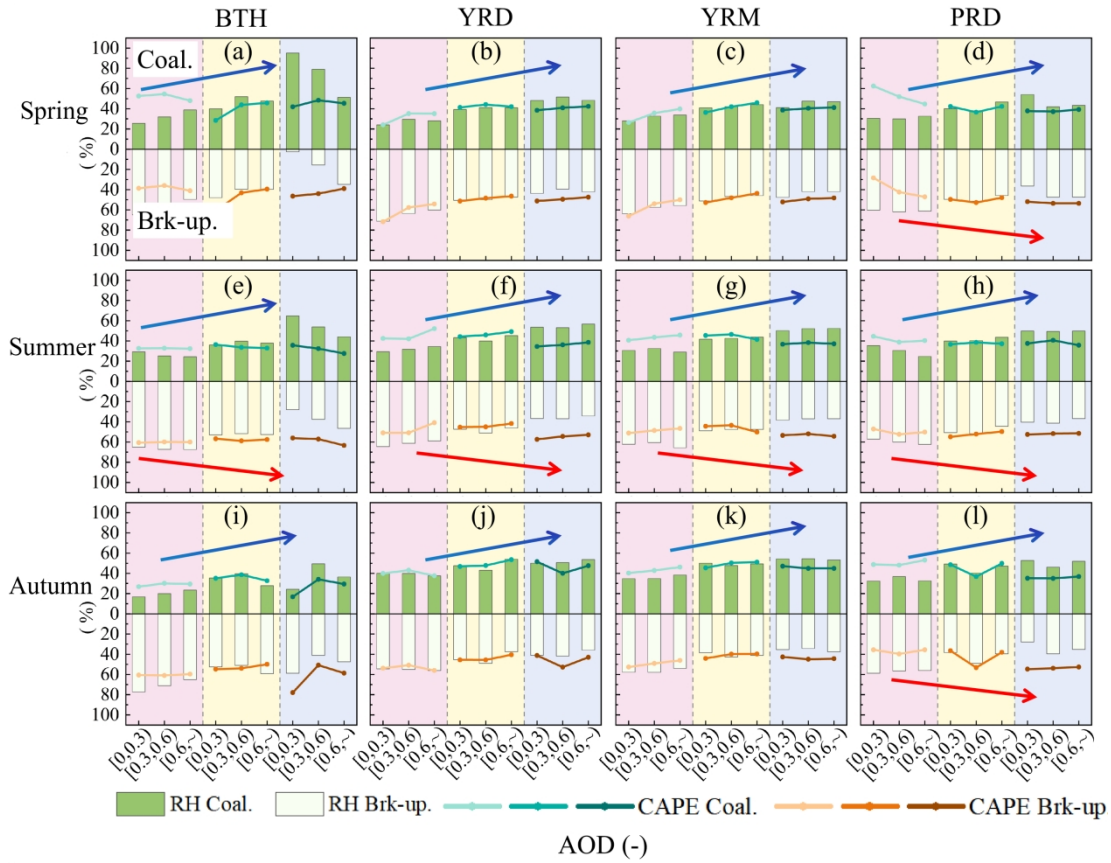

Fig. S22. Stratiform precipitation coalescence and break-up processes under varying RH and CAPE conditions in spring (a–d), summer (e–h), and autumn (i–l) across regions sorted by AOD loading. The form of this expression is similar to that shown in Fig. S9.